

A Comparative Analysis of Spectral Reflectance Reconstruction in Various Spaces Using a Trichromatic Camera System

Francisco H. Imai and Roy S. Berns
Munsell Color Science Laboratory, Rochester Institute of Technology
Rochester, New York, USA

Abstract

An analysis is presented of how the space in which principal component analysis is performed can affect the colorimetric and spectral accuracy of spectral reconstruction. The spectral reconstruction is performed using digital counts given by a new concept of spectral image acquisition constituted by a trichromatic camera combined with absorption filters, instead of the traditional monochrome camera and a set of interference filters. The comparison of the spectral reconstruction performance in each space shows the advantages and disadvantages of using alternative spaces rather than reflectance.

Introduction

During the last Color Imaging Conference we introduced an image capturing system that results in spectral image archives with sufficient spatial resolution and colorimetric accuracy for artwork imaging.[1,2] In this system, a multi-band, low-spatial resolution multi-spectral image is combined with a high-spatial resolution lightness image (from either a monochrome digital camera or digitized photograph) to generate a high-spatial resolution spectral image. This will greatly reduce the cost and complexity of the image acquisition system. At the same time, this system enables defining images spectrally and the use of spectral information in order to provide printed color reproductions that are close spectral matches to the original objects. Thus, it produces high-quality color matching under different illuminations and observers. This method applies *a priori* spectral analysis, linear modeling techniques, and exploiting of the human visual system's spatial properties to achieve high-resolution multi-spectral images. Preliminary experiments of this method showed promising results.

Technical issues concerned with multi-spectral image acquisition have been studied intensively.[1-23] We also have been studying an alternative way to capture multi-spectral images using a conventional trichromatic digital camera combined with absorption filters[1,3] in order to overcome the inherent limitations of a traditional monochrome camera combined with interference filters.[8,9] Our goal in this research has focused on reducing the cost and complexity of the image acquisition system while preserving its colorimetric and spectral accuracy.

Traditionally, the spectral reconstruction from digital camera signals has been performed in reflectance space, because digital camera signals are directly related to spectral reflectance. When dealing with other spaces rather than reflectance, *e.g.* absorption, absorption vectors and digital count vectors are not in the same space and a non-linear transformation should be performed *a priori* to produce digital counts directly related to the space. This digital count transformation enables the use of principal component analysis and other linear tools.

This contribution will focus on the analyses of the spectral reconstruction performed in various spaces, besides reflectance, using transformed normalized signals from a trichromatic camera combined with absorption filters. In this research, we will compare the performance of spectral reconstruction by principal component analysis in reflectance space, Kubelka-Munk (K/S) space for opaque materials, and a new empirical space proposed by Tzeng and Berns[21] that gives a near-normal and reduced dimensionality space for subtractive opaque processes. Using different targets and combinations of trichromatic signal sets, we will analyze the influence of the database used for principal component analysis, and the filtering on the accuracy of the results given by the spectral reconstruction in each considered space.

Technical Approach

The spectral reflectance of each pixel of a painting can be estimated using *a priori* spectral analysis with direct measurement and imaging of color patches to establish a relationship between the digital counts and spectral reflectance.

A set of spectral reflectances, $\mathbf{r}$, is measured and then the corresponding set of eigenvectors, $\mathbf{e}$, is calculated by principal component analysis. Then, the set of eigenvalues, α, corresponding to the eigenvectors, $\mathbf{e}$, are calculated using the spectral reflectances, $\mathbf{r}$. A relationship between digital counts, $\mathbf{C}$, and eigenvalues, α, can be established by the equation

$$\mathbf{A} = \alpha\mathbf{C}^{\mathbf{T}}[\mathbf{C}\mathbf{C}^{\mathbf{T}}]^{-1} \quad (1)$$

where $\mathbf{T}$ denotes transpose matrix.

The matrix $\mathbf{A}$ can be used to calculate the eigenvalues, α, from digital counts to reconstruct the spectral reflectance.

Spaces to Perform Principal Component Analysis

I) Reflectance Space

Reflectance space is directly related to the digital counts of the digital camera and it is traditionally used to perform spectral analysis.

II) Kubelka-Munk Space

Reflection, absorption and scattering occur when opaque surfaces are exposed to light. Kubelka and Munk proposed a turbid media theory that derives the relationship between reflectance factor, absorption and scattering.[23] According to Kubelka-Munk formulation, reflectance factor is a function of the absorption and scattering ratio **(K/S).** The Kubelka-Munk equations relating reflectance factor, $\mathbf{R}$, and the ratio, **(K/S)**, of absorption and scattering for opaque materials are given by equations (2) and (3).

$$(\mathbf{K}/\mathbf{S}) = \frac{(1-\mathbf{R})^2}{2\mathbf{R}} \quad (2)$$

$$\mathbf{R} = 1 + (\mathbf{K}/\mathbf{S}) - \sqrt{(\mathbf{K}/\mathbf{S})((\mathbf{K}/\mathbf{S})+2)} \quad (3)$$

In Kubelka-Munk space the ratio **(K/S)** of absorption and scattering is approximately linear with respect to colorant concentration.[24]

III) New Empirical Space

Tzeng and Berns proposed a new empirical space that gives a near-normal and reduced dimensionality for subtractive opaque processes.[21] The transformations from reflectance factor, $\mathbf{R}$, to the new space, Ψ, are given by equations (4) and (5), where **a** is an offset vector which is empirically derived.

$$\Psi = \mathbf{a} - \sqrt{\mathbf{R}} \quad (4)$$

$$\mathbf{R} = (\mathbf{a} - \Psi)^2 \quad (5)$$

Experiments

In our experiments, we considered one imaging system, three targets, images captured using combinations of three sets of trichromatic signals, and principal component analysis performed in three different spaces. For imaging systems, we used a high-resolution IBM PRO\3000 digital camera system (3,072 x 4,096 pixels, 12 bits per channel). The spectral sensitivities of the camera were measured, as well as the spectral radiant power of the illuminant used in the imaging. A GretagMacbeth ColorChecker and two sets of painted patches were imaged (one of them made by acrylic paints and the other by post-color paints). The different combinations of trichromatic signals were obtained from the trichromatic data without filtering, the trichromatic data with a light-blue filter (Kodak Wratten filter number 38), and a very-light-green filter (Kodak Wratten filter number 66).

I. Performance of Principal Component Analysis in Different Spaces

In this simulation, a statistical analysis was performed without introducing noise in the digitizing system. The spectral reflectances of the GretagMacbeth ColorChecker and two sets of painted patches were measured. Kubelka-Munk, (K/S), and the new empirical space, ψ, were calculated from the measured reflectances. Principal component analysis was performed in each space. As an example, Table I shows the influence of the number of eigenvectors on the colorimetric accuracy using CIE94 (D50 and 2° observer) and on the spectral accuracy of the estimation for the set of 147 painted patches produced using mixtures of GALERIA acrylic colorant produced by Winsor & Newton (Cadmium Red Hue, Permanent Green Deep, Ultramarine, Cerulean Blue Hue, Permanent Magenta, Cadmium Yellow Medium Hue, Mars Black and White).

Analyzing the overall simulation results of all three targets, the spectral reconstruction in the new empirical space presented slightly better spectral and colorimetric accuracy than the reconstruction in the reflectance space. Table I shows that, if we use a trichromatic digitizing system to capture images, at least 6 eigenvectors, corresponding to 2 sets of trichromatic signals, are needed to produce accuracy of ΔE^*_{94} less than a unity and spectral reflectance rms error of less than 2.5%.

II. Estimation of Spectral Reflectance Using Simulated Digital Counts

One can simulate the digital counts using a camera model given by $\mathbf{C}=(\mathbf{DF})^{\mathrm{T}}\mathbf{Sr}$, where $\mathbf{D}$ is the camera spectral sensitivities, $\mathbf{F}$ is the spectral transmittance of the filters, $\mathbf{S}$ is the illumination spectral power distribution, $\mathbf{r}$ is the object spectral reflectance, and $\mathbf{C}$ is the simulated digital counts. The estimation of the spectral reflectance using simulated digital counts gives a performance of the estimation of reflectance for each target, for each trichromatic signal combination, in each space, without introducing noise from the real, measured digital counts. The digital counts do not have direct proportionality with Kubelka-Munk and the new empirical spaces.

In order to solve this problem, transformations for the digital counts were derived, in the same way defined in equations (2) and (4), by equations (6) and (7), for Kubelka-Munk and the new empirical spaces, respectively.

$$\mathbf{C}' = \frac{1}{2\mathbf{C}} + \frac{\mathbf{C}}{2} - 1 \quad (6)$$

$$\mathbf{C}' = 1 - \sqrt{\mathbf{C}}, \quad (7)$$

where $\mathbf{C}'$ is the transformed digital count and $\mathbf{C}$ is the normalized digital count.

Table I. Influence of the number of eigenvectors in each space used in the spectral reconstruction on the colorimetric and spectral error for a set of painted patches produced using acrylic paints.

Number of Eigenvectors	Reflectance space		Kubelka-Munk space	
	Mean ΔE^*_{94}	Reflectance factor rms error	Mean ΔE^*_{94}	Reflectance factor rms error
1	26.6	0.140	23.3	0.171
2	15.6	0.068	15.5	0.078
3	4.1	0.027	1.9	0.050
4	1.3	0.016	1.6	0.030
5	0.7	0.012	1.2	0.033
6	**0.4**	**0.009**	**0.9**	**0.022**
7	0.3	0.007	0.4	0.019
8	0.2	0.005	0.3	0.022
9	0.1	0.004	0.2	0.016
10	0.05	0.002	0.2	0.017
11	0.02	0.001	0.2	0.017
12	0.01	0.001	0.2	0.014

Number of Eigenvectors	New empirical space	
	Mean ΔE^*_{94}	Reflectance factor rms error
1	32.7	0.192
2	13.6	0.068
3	3.3	0.025
4	1.0	0.013
5	0.5	0.009
6	**0.3**	**0.007**
7	0.2	0.006
8	0.1	0.004
9	0.03	0.003
10	0.02	0.002
11	0.01	0.001
12	0.00	0.001

As a result of the simulations, it was possible to observe that the non-linear transformations given by equations (6) and (7) improved the accuracy of the spectral reconstructions. The simulations in Kubelka-Munk space produced spectral mismatches and large colorimetric errors for patches with high reflectance factors. High reflectance factors produce very small (K/S) values. When spectral reconstruction is performed using principal component analysis in reduced dimensionality, there is an error in the reconstruction that can produce negative (K/S) values. When these negative values are introduced in equation (3) we have negative values in a square root. For example, Figure 1a shows the comparison of the measured and estimated spectral reflectance of the Orange-Yellow patch of the GretagMacbeth ColorChecker reproduced using 6 eigenvectors and 6 signals in Kubelka-Munk space. It shows a considerable mismatch in the high reflectance factor region of the spectrum. However, the estimation in Kubelka-Munk space produced very good results for some patches with low reflectance factors, that was not reproduced well in reflectance space, such as the Purple patch of the GretagMacbeth ColorChecker. Figure 1b shows the comparison of the measured and estimated spectral reflectance of the Purple patch reproduced using 6 eigenvectors and 6 signals in reflectance space. Figure 1c shows the comparison of the measured and estimated spectral reflectance of the purple patch reproduced using 6 eigenvectors and 6 signals in Kubelka-Munk space.

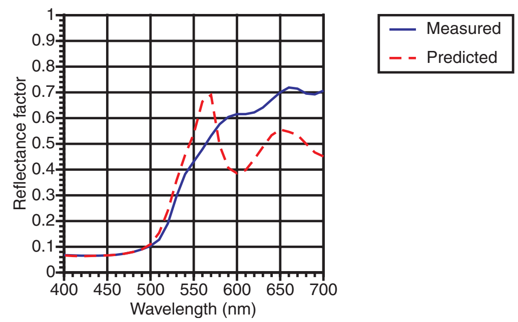

a) ColorChecker Orange-Yellow match in Kubelka-Munk space.

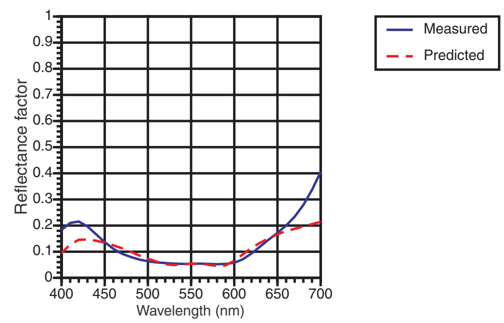

b) ColorChecker Purple match in reflectance space.

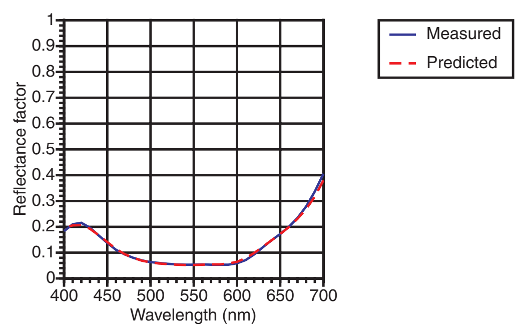

c) ColorChecker Purple match in Kubelka-Munk space.

Figure 1. Comparisons of measured and predicted spectral reflectances using 6 eigenvectors and 6 signals: trichromatic signal without filter and trichromatic signal with Wratten absorption filter number 38 (light blue).

In all of the estimations above, the 6 camera signals were derived using trichromatic signals without filter and trichromatic signals with Kodak Wratten absorption filter number 38 (light blue) and the spectral sensitivities of IBM PRO\3000 digital camera system.

Analyzing the performance in the reflectance, K/S and new empirical spaces it was possible to see the dependency on the database used to perform principal component analysis. Both reflectance and the empirical spaces produced, in general, acceptable results. In this paper, we will present the results of the spectral estimation from digital counts for the IBM Digital Camera System with 6 eigenvectors and 6 signals (given by R, G, B without filtering and R, G, B with Kodak Wratten absorption filter number 38) in the new empirical space, because this combination produced the best overall colorimetric and spectral accuracy. The result for simulated digital counts of the GretagMacbeth ColorChecker in the empirical space is summarized in Table II. ΔE^*_{94} and ΔE^*_{ab} calculations were performed for illuminant D50 and 2° observer. The metameric index was calculated using the Fairman metameric black method, between standard illuminants D50 and A using ΔE^*_{94} in the calculations.[25]

Table II. Spectral reconstruction of GretagMacbeth ColorChecker using 6 eigenvectors in new empirical space for 6 signals: R, G, B without filter and R, G, B with Wratten absorption filter number 38 (light blue).

Results	ΔE^*_{ab} (D50, 2°)	ΔE^*_{94} (D50, 2°)	Reflectance factor rms error	Metameric index (ΔE^*_{94}) (D50, A)
Mean	**1.7**	**0.9**	**0.020**	**0.4**
Standard Deviation	0.9	0.4	0.009	0.3
Max	4.0	2.4	0.043	1.0
Min	0.5	0.5	0.006	0.05

III. Estimation of the spectral reflectance using measured digital counts

This estimation applies basically the same idea of the linear method using simulated digital counts, but instead of simulated digital counts using a camera model, spectral reflectance is estimated from measured digital counts averaged over each imaged patch. Tables III, IV and V shows the colorimetric and spectral accuracy for spectral reconstruction in the empirical space using trichromatic signals for the same conditions of Table II for IBM Pro\3000 digital camera system, for the GretagMacbeth ColorChecker, the acrylic painted patches and the post-color painted patches, respectively.

Comparing the results of the spectral reconstruction for the GretagMacbeth ColorChecker summarized in Tables II and III, the averaged colorimetric differences were worse in the reconstruction using measured digital counts than the reconstruction using simulated digital counts by a factor of about 2. The reflectance rms error factor was about 50% worse in the reconstruction using measured digital counts than the reconstruction using simulated digital counts. This result was expected because of the introduction of noise and typical experimental error. However, our results obtained for the spectral reconstruction of the GretagMacbeth ColorChecker with color difference ΔE^*_{ab} of 2.9 is better than the average ΔE^*_{ab} of 4.0, obtained using a monochrome digital camera and a set of 7 interference filters by Burns.[16] Our results are also similar to the ΔE^*_{ab} between 2 and 3 (depending on the lighting used to image) obtained by the MARC camera in the VASARI project (though this system was optimal for colorimetric performance and does not estimate spectral data).[26]

Table III. Spectral reconstruction of GretagMacbeth ColorChecker using 6 eigenvectors in new empirical space for 6 signals: R, G, B without filter and R, G, B with Wratten absorption filter number 38 (light blue).

Results	ΔE^*_{ab} (D50, 2°)	ΔE^*_{94} (D50, 2°)	Reflectance factor rms error	Metameric index (ΔE^*_{94}) (D50, A)
Mean	**2.9**	**1.9**	**0.029**	**0.8**
Standard Deviation	1.8	0.9	0.013	0.5
Max	7.5	3.5	0.066	2.0
Min	0.5	0.6	0.005	0.1

Table IV. Spectral reconstruction of acrylic painted patches using 6 eigenvectors in new empirical space for 6 signals: R, G, B without filter and R, G, B with Wratten absorption filter number 38 (light blue).

Results	ΔE^*_{ab} (D50, 2°)	ΔE^*_{94} (D50, 2°)	Reflectance factor rms error	Metameric index (ΔE^*_{94}) (D50, A)
Mean	**4.2**	**3.1**	**0.027**	**1.3**
Standard Deviation	2.8	2.3	0.015	1.1
Max	24.1	17.5	0.076	6.4
Min	0.2	0.1	0.003	0.04

Table V. Spectral reconstruction of post-color painted patches using 6 eigenvectors in new empirical space for 6 signals: R, G, B without filter and R, G, B with Wratten absorption filter number 38 (light-blue).

Results	ΔE^*_{ab} (D50, 2°)	ΔE^*_{94} (D50, 2°)	Reflect factor rms error	Metameric index (ΔE^*_{94}) (D50, A)
Mean	**3.3**	**1.9**	**0.025**	**1.0**
Standard Deviation	2.1	1.5	0.010	0.7
Max	11.8	8.9	0.055	4.8
Min	0.4	0.3	0.008	0.03

Conclusion

The experimental sequence of the spectral reconstruction from trichromatic digital camera combined with absorption filters was described, showing, at first, the colorimetric and spectral accuracy predicted by statistical analysis of samples, and progressively adding noise, first calculating the simulated digitizing camera system, and finally, presenting the performance of the reconstruction using measured digital counts from imaged patches. As a result, the spectral reconstruction in the new empirical space using a combination of trichromatic signals without filtering and with light blue absorption filter produced the best overall colorimetric and spectral performance for the three targets we analyzed. Spectral reconstruction using higher order estimation could produce better results. However, six eigenvectors in the empirical space presents a compromise between accuracy and fulfillment of our goals of simplicity and cost reduction. Furthermore, the average colorimetric result of our reconstruction for the GretagMacbeth ColorChecker were better or similar to other spectral reconstruction systems using traditional techniques with the advantage of simplifying the imaging system.

Although spectral estimation in Kubelka-Munk (K/S) space produced suitable spectral matches for colorants with low reflectance factors, it can produce unacceptable errors when reducing the dimensionality in principal component analysis. Therefore, this space is not recommended for the spectral estimation of artwork images unless iterative methods are incorporated (e.g. references 27 and 28).

References

1. F. H. Imai and R. S. Berns, High-resolution Multi-Spectral Image Archives: A Hybrid Approach, *Proc. of The Sixth Color Imaging Conference: Color Science, Systems, and Applications*, pg. 224, (1998).
2. R. S. Berns, F. H. Imai, P. D. Burns and Di-Y. Tzeng, Multi-spectral-based color reproduction research at the Munsell Color Science Laboratory, *Proc. of SPIE Europto Series,* Vol. **3409**, pg. 14, (1998).
3. F. H. Imai and R. S. Berns, Spectral Estimation Using Trichromatic Digital Cameras, *Proc. of the International Symposium on Multispectral Imaging and Color Reproduction for Digital Archives, in press,* (1999).
4. R. S. Berns, Challenges for color science in multimedia imaging, *Proc. CIM'98 Colour Imaging in Multimedia*, University of Derby, pg. 123, (1998).
5. J. Y. Hardeberg, F. Schmitt, H. Brettel, J-P. Crettez and H. Maitre, Multispectral imaging in multimedia, *Proc. CIM'98 Colour Imaging in Multimedia*, University of Derby, pg.75, (1998).
6. S. Baronti, A. Casini, F. Lotti and S. Porcinai, Multispectral imaging system for the mapping of pigments in works of art by use of principal-component analysis, *Applied Optics* **37**, 1229, (1998).
7. H. Maitre, F. J. M. Schmitt, J-P. Crettez, Y. Wu and J. Y. Hardeberg, Spectrophotometric image analysis of fine art paintings, *Proc. IS&T/SID Fourth Color Imaging Conference: Color Science, Systems and Applications*, pg. 50, (1996).
8. F. Köig and W. Præfke, The practice of multispectral image acquisition, *Proc. SPIE* **3409**, pg. 34, (1998).
9. F. Köig and W. Præfke, A multispectral scanner, *Proc. CIM'98 Colour Imaging in Multimedia*, University of Derby, pg. 63, (1998).
10. Y. Miyake, Y. Yokoyama, N. Tsumura, H. Haneishi, K. Miyata and J. Hayashi, Development of multiband color imaging systems for recording of art paintings, *Proc. SPIE* **3648**, pg. 218 (1999).
11. S. Tominaga, Spectral Imaging by a Multi-Channel Camera, *Proc. of SPIE* **3648,** pg. 38 (1999).
12. H. Haneishi, T. Hasegawa, N. Tsumura and Y. Miyake, Design of color filters for recording artworks, *IS&T's 50th Annual Conference*, pg. 369, (1997).
13. M. J. Vrhel and H. J. Trussel, Color correction using principal components, *Color Res. Appl.* **17**, 26, (1992).
14. D. S. S. Vent, *Multichannel analysis of object-color spectra*, Master Degree Thesis, RIT, 1994.
15. W. Præfke and T. Keusen, Optimized basis functions for coding reflectance spectra minimizing the visual color difference, *Proc. IS&T/SID 1995 Color Imaging Conference: Color Science, Systems and Applications*, pg. 37, (1995).
16. P. D., Burns, *Analysis of image noise in multi-spectral color acquisition*, Ph. D. Thesis, R.I.T., 1997.
17. W. Præfke, Analysis-synthesis transforms versus orthogonal transforms for coding reflectance spectra, *Proc. IS&T/SID 5th Color Imaging Conference: Color Science, Systems and Applications*, pg. 177, (1997).
18. F. Köig, Reconstruction of natural spectra from a color sensor using nonlinear estimation methods, *Proc. IS&T's 50th annual conference*, pg. 454, (1997).
19. P. D. Burns and R. S. Berns, Error propagation analysis in color measurement and imaging, *Color Res. Appl.* **22**, 280, (1997).
20. M. J. Vrhel, R. Gershon and L. S. Iwan, Measurement and analysis of object reflectance spectra, *Color Res. Appl.* **19**, 4, (1994).
21. D-Y. Tzeng and R. S. Berns, Principal Component Analysis for Color Science Applications, (submitted to Color Research and Application).
22. F. Köig and P. G. Herzog, On the Limitations of Metameric Imaging, *Proc. of IS&T PICS Conference,* pg. 163, (1999).
23. P. Kubelka, New contribution to the optics of intensely light-scattering materials. Part I. *J. Opt. Soc. of Am.* **38**, 448 (1948).
24. E. Allen, Basic equation used in computer color matching, *J. of Opt. Soc. of Am.* **56**, 1256, (1966).
25. H. S. Fairman, Metameric correction using parametric decomposition, *Color Res. Appl.,* **12**, 261, (1997).
26. J. Cupitt, D. Saunders and K. Martinez, Digital imaging in European museums, *Proc. of SPIE* **3025**, pg. 144, (1997).
27. M. A. Rodriguez and T. G. Stockham, Producing colorimetric data from densitometric scans, *Proc. SPIE* **1913**, pg. 413, (1993).
28. R. S. Berns and M .J. Shyu, Colorimetric characterization of a desktop drum scanner using a spectral model, *J. Electronic Imaging* **4**, 360, (1995).